THE BELL SYSTEM TECHNICAL JOURNAL
Vol. 62, No. 7, September 1983
Printed in U.S.A.

Empirical Evaluation of Profile Variations in an MCVD Optical Waveguide Fiber Using Modal Structure Analysis

By A. CARNEVALE* and U. C. PAEK†

(Manuscript received November 15, 1982)

This paper presents a computer modeling evaluation of the effect on mode propagation of typical perturbations in the refractive index profile produced as a result of the MCVD process. Certain profile variations were eliminated, singly and/or collectively, and the resultant changes in modal structure analyzed. The most important factor in the deterioration of the bandwidth is the presence of a refractive index dip at the core center. Small shifts in the level of dopant were seen to broaden pulse shapes and thus reduce bandwidth. Much less effect on bandwidth is associated with the ripples in the profile, as is also true for dips in refractive index below the index of the cladding near the core-cladding interface. A perpendicular rise, or step, in index of refraction at the core-cladding interface reduces the number of altered modes near the cladding.

I. INTRODUCTION

In a previous paper[1] we reported on calculation of the modal structure as a function of wavelength (λ) of an optical waveguide produced by the Modified Chemical Vapor Deposition (MCVD) process using an exact numerical procedure. This technique[2] has been used extensively to investigate various theoretical aspects of optical waveguide propagation.[3-6] We observed excessive splitting and scattering in the

* Bell Laboratories. † Western Electric.

effective indices (N_e) and the group indices (N_g), which lead to a reduction of the bandwidth (BW) at any particular λ.[1] We concluded that the profile variations inherent in the MCVD process were responsible for the reduction of the BW. This paper analyzes in detail the same profile considered there.

The profile is shown in Fig. 1. The data, obtained by the laser beam refraction method,[7] indicates the change in refractive index (ΔN_r) as a function of the unnormalized radius (r). $\Delta N_r = 0$ corresponds to the cladding, in this case, SiO_2. The major deviations (imperfections) of this MCVD profile from a power law (α) profile are common to most profiles produced by the MCVD process. These include:

1. Region A in the plot, usually referred to as "BURNOFF" or "BURNOUT", which indicates a precipitous reduction in the refractive index at the core center. This reduction is believed to be due to the vaporization of dopant components, such as GeO_2, during the high-temperature collapse phase of the process.

2. Region B, which extends over most of the profile, containing what are generally called "RIPPLES", whose width and amplitude

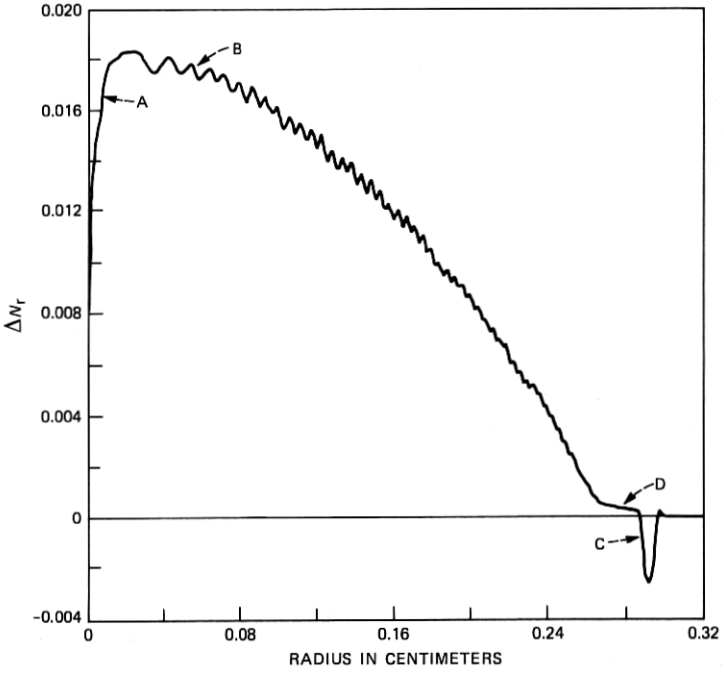

Fig. 1—MCVD profile. The region A denotes the burnout while the region B, which extends over most of the profile, shows the characteristic ripples referred to in the text. Regions C and D refer to the dip and the step, respectively. The radius data are not normalized.

increase toward the core center. These ripples are a direct result of the compositional gradient across the MCVD layer, burnoff of GeO_2 at the surface of the layer, and the finite number of discrete layers of changing composition (typically 50).

3. The sharp "DIP", C, near the core-cladding interface caused by the use of an index-reducing dopant in the deposited barrier layer, in this case, boron. In some special cases this "depressed cladding" feature can have a greater width than shown.

4. The "STEP", D, at the cladding.

The above deviations constitute the major obvious perturbations of the MCVD profile from an ideal profile. More subtle deviations, which are usually ignored, will be seen later in this report.

II. METHOD

It was deemed necessary and sufficient to find the effective indices and the group indices for the:

1. Meridional modes $TE_{0,q}$, and $TM_{0,q}$
2. Helical modes $HE_{1,q}$, and $EH_{1,q}$ over some wavelength region of interest.

The subscripts above denote the angular and radial mode number (m, q) respectively. Thus we conducted the modeling process at 11 specific wavelengths itemized below in Table I.

2.1 "As is" case

Initially, N_e and N_g of the modal groups at $m = 0$ and $m = 1$, were obtained for each of the λ's listed in Table I, operating on the MCVD profile as it exists; i.e., on an "as is" basis. Figure 2 shows examples of the distribution of N_g vs N_e for $\lambda = 0.82$ (a), 1.32 (b), and 1.55 (c) μm, respectively. We note the counterclockwise rotation of the data as a function of increasing λ; this rotation has been commented on in our early work.[4] The profile was shown to remain constant with λ, but the group index vs effective index changes in this manner owing to the dependence of bandwidth on α.

We further note the clear separation (splitting) of the HE modes (Δ) from all other modes (○, ●); this separation decreases as λ increases. The two groups appear to be moving roughly in parallel but

Table I—Wavelengths used for modeling process

Test No.	1	2	3	4	5	6	7	8	9	10	11
Wavelength (μm)	0.6328*	0.70	0.82*	0.90	1.00	1.10	1.20	1.23	1.32*	1.40†	1.55*

* Of current interest in engineering applications. All others listed are solely for the purpose of parameterizing the MCVD deviations from an ideal profile, as a function of wavelength, if possible.

† Water peak.

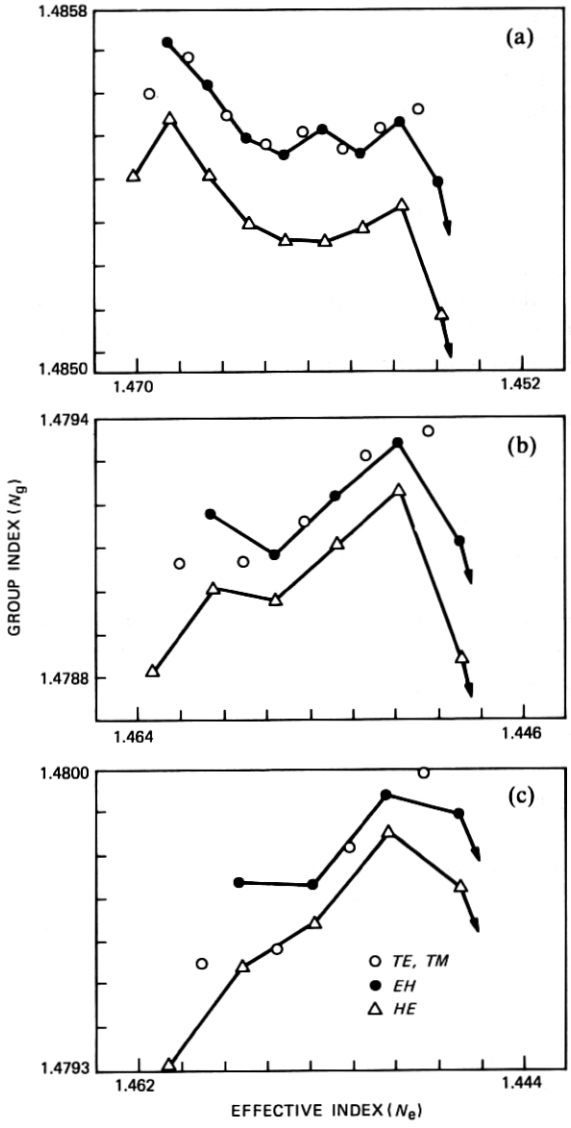

Fig. 2—N_g vs N_e—"as is" case. (a) $\lambda = 0.82$ μm. (b) $\lambda = 1.32$ μm. (c) $\lambda = 1.55$ μm.

displaced in time. This can result in two or more peaks, depending on any mode mixing, in the output pulse of the fiber, and a reduction in the BW at any λ. BW reduction would be more severe at short λ's, where the splitting is greater. Last, we observed the drop-off (lower N_g) of those high-order modes near the cladding. These modes have been altered because of their proximity to the cladding. The plots of

Fig. 2 can be compared to the ideal case of a power law profile using the computed α, ΔN, and r derived from the MCVD profile.[1] A plot of N_g at each λ results in a shape similar to those shown in the MCVD plot by (○, ●); i.e., other than the *HE* (Δ) modes.

2.2 *"No ripple or dip" case*

To analyze the effect of the MCVD imperfections on the modal structure, each was removed separately. Our first step was to remove the ripple in the section (B) between the burnout (A) and the step (D) in Fig. 1. Past experience in α curve fitting to MCVD profiles indicated that rarely can one fit section B with a single α. Because we did not want to destroy any short-term (local) variations in ΔN and/or α, we partitioned the B region into eight equal radial segments, and fitted each segment with a least squares parabola. We then used the fitted curve as the profile in each segment. The index of refraction data shown in Fig. 1 is collected at a number of discrete points and is generally not a continuous curve.

Next, the dip (C) was removed by connecting the end points with a two-point straight line, thus making the step (D) continuous. This correction caused negligible change in the spectrum and so for brevity we eliminated the ripple and dip in one operation.

One example, which is typical of all λ's tested, is given in Fig. 3 at $\lambda = 0.6328$ μm. Figure 3a is the modal display on an as is basis, while Fig. 3b is the result for no ripple or dip. The as is plot is consistent with those λ's shown in Fig. 2, i.e., the rotation of the data, the drop-off of the high-order modes, and, most important, the splitting of *HE* from all other modes. The relatively short λ of 0.6328 μm makes the N_e and N_g very sensitive to the short-term variations in the profile. We see the development of some jagged peaks and depressions in the display as we approach the cladding. Since it is the high-order modes that are most affected, imperfections in the profile near the cladding are most likely responsible for the development of these sharp features. It could be the step D, or as seems more likely, a shift in α or ΔN in the latter part of section B in the profile. Identification of the parameter responsible (ΔN or $\Delta\alpha$) is difficult. In any case, a change in either results in shifting N_g in the same direction. We can see two pronounced shifts at $r = 18$ and $r = 22$ in Fig. 1. If we examine the fine structure of the profile, we can detect other such shifts over the full range of the radius. Although these shifts appear to be small, they can cause large changes in the eigenvalues and, thereby, in N_g. We can therefore associate the ragged appearance of N_g in our plots with very small changes in ΔN_r.

Elimination of the ripple and the dip (Fig. 3b) reduces the scatter of the data and lessens the effect of the shifts in ΔN, probably because

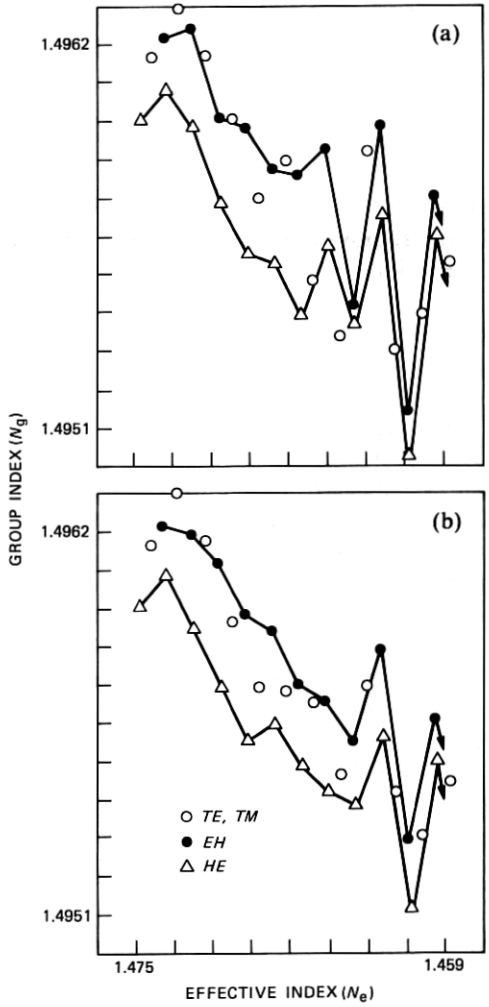

Fig. 3—Plot of N_g vs N_e for $\lambda = 0.6328$ μm. (a) "As is" case. (b) Ripple and dip removed.

it acts as a smoothing mechanism. However, it does not eliminate or reduce the separation of the *HE* modes and therefore is not the major cause of reduced BW resulting from this profile. The data in Figs. 3a and b appear to have approximately the same slope, but the slope in Fig. 3b is more clearly defined, probably as a result of the smoothing action.

2.3 "No burnout" case

The next MCVD deviation eliminated was the dip in the index of refraction at the core center, i.e., the burnout region (A) in Fig. 1. To

accomplish this, we found the maximum ΔN in the profile and extended it in a horizontal line to the core center. The rest of the profile was kept intact, thus preserving the original ripples, dip, and step. Figure 4 shows the results at $\lambda = 1.23$ μm. Figure 4a shows the results on an as is basis, while Fig. 4b shows the case without burnout.

The as is result at this λ is again consistent with our earlier results. At this longer λ, N_e and N_g are much less sensitive to the short-term variations in the profile, which is evident in the relatively smooth plot of N_g vs N_e as compared to the same plot (Fig. 3a) at $\lambda = 0.6328$ μm.

The elimination of the burnout (Fig. 4b) has removed the displacement in time of the *HE* modes and all modal groups are now traveling together. This remarkable result was observed at all λ's (see Table I) tested. Except for considerations of α optimum (α_{opt}), the burnout appears to be of paramount significance in the deterioration, or optim-

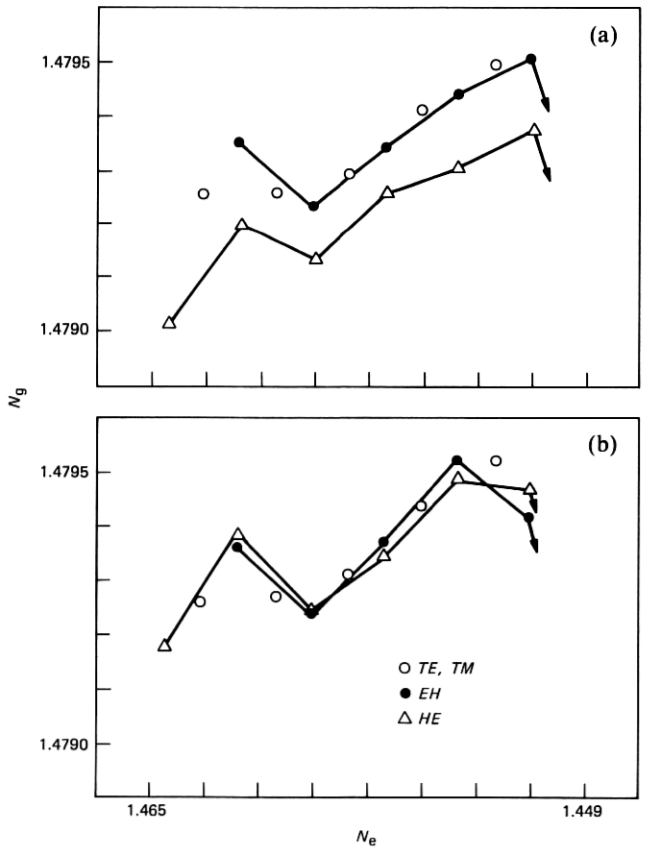

Fig. 4—N_g vs N_e for $\lambda = 1.23$ μm. (a) "As is" case. (b) "No burnout" case.

ization, of the BW. We should realize that the burnout region in this MCVD profile is much less than that seen in most MCVD profiles.

2.4 *"Inverted burnout" case*

Because of the previous results we decided to investigate a phenomenon sometimes seen in MCVD profiles. This defect can occur as a result of overcompensation of dopant in attempting to reduce or eliminate burnout. A study of some MCVD profiles[8] in which this defect was present indicated that we could simulate this characteristic by simply inverting the burnout. We found the difference of ΔN from the maximum ΔN and added this difference to the maximum, over the burnout region A in Fig. 1.

Figure 5 shows one result at $\lambda = 1.20$ μm, which was typical of all

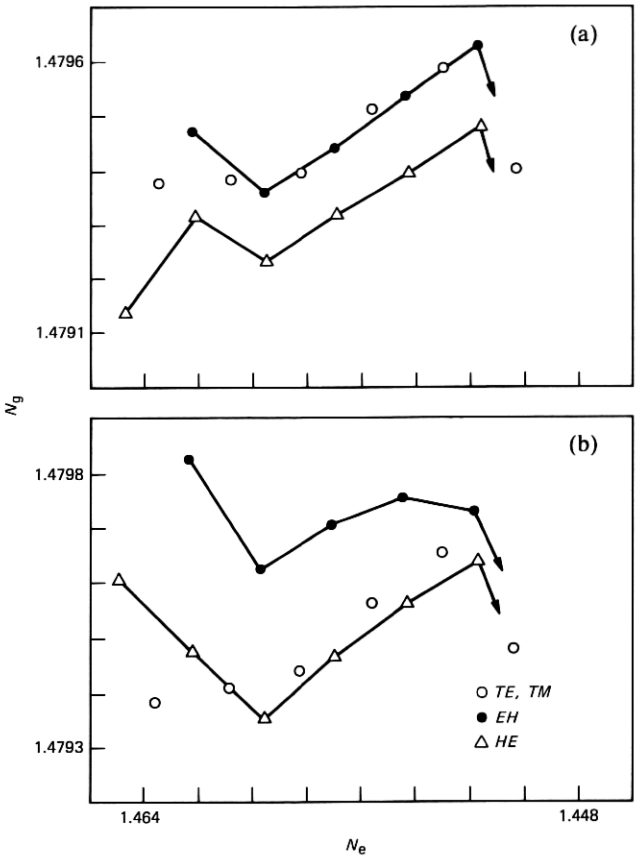

Fig. 5—N_g vs N_e for $\lambda = 1.20$ μm. (a) "As is" case. (b) "Inverted burnout" case.

λ's tested. Figure 5a is the modal display on an as is basis (which includes the burnout), and Fig. 5b is the result for the inverted burnout (overcompensation).

The as is result is consistent with our previous observations on similar spectra at other λ's.

Inverting the burnout (Fig. 5b) has displaced the *EH* modes from all the rest, and further, this displacement is much greater than the burnout effect, and thus is far more serious than burnout in the decrease of the BW. Our calculations indicate that if both burnout and overcompensation are present simultaneously (which has been observed at times), both splittings would also occur, i.e., the two effects would not be cancelled). Thus we would expect three or more peaks, depending on mode mixing, in the output pulse of the fiber.

2.5 "No step" case

One last perturbation in the MCVD profile remains to be examined, namely, the step (D) near the cladding. We used the least squares fitted curve for the ripple section of the profile nearest the step. We eliminated the step D (and also the dip C) by using the derived equation to extrapolate paired values of r, ΔN_r to the cladding. At $\Delta N_r = 0$, the radius is then renormalized to 25 μm. One comprehensive result is given in Fig. 6 at $\lambda = 0.70$ μm, where all plots are on identical scales and are called:

1. As is
2. No ripple or dip
3. No ripple, dip or burnout
4. No ripple, dip, burnout, or step.

The as is modal display (A) is consistent with our previous observations at other λ's on this basis. We see the separation of the *HE* modes due to the burnout and the increased sensitivity to the short-term variations in this profile at this relatively short λ. We note the development of the sharp features in the distribution as we approach the cladding; this is very similar to the comparable spectrum (Fig. 3a) at $\lambda = 0.6328$ μm.

Removing the ripple and dip (Fig. 6b) provides the same smoothing mechanism previously cited (see Fig. 3b for example).

Figure 6c is the modal distribution realized when the ripple, dip, and burnout have been removed, retaining the step. We see that all modes are now travelling together (no *HE* separation), and that we are now approaching the distribution to be realized for an ideal profile, except for the short-term shifts in ΔN_r in the profile.

Figure 6d is the modal distribution obtained when the ripple, dip, burnout, and step have been eliminated. This distribution represents the closest approach to an ideal profile. The severe drop-off in N_g of

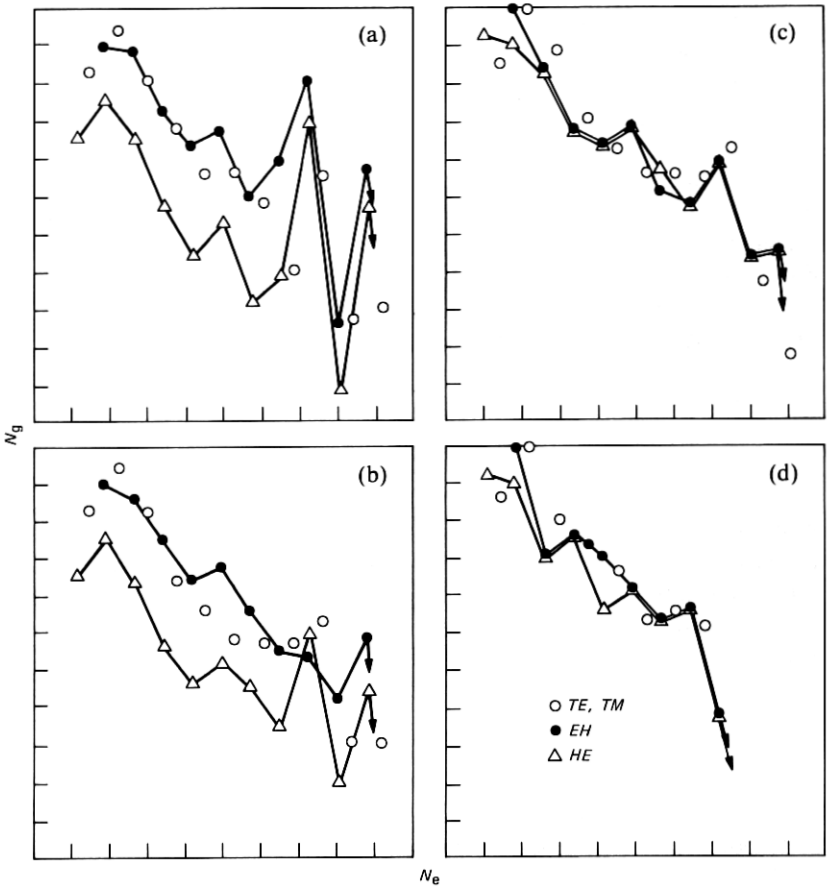

Fig. 6—N_g vs N_e for $\lambda = 0.70$ μm (Scales are identical in all sections). (a) "As is" case. (b) No ripple or dip case. (c) No ripple, dip, or burnout (step is in). (d) No ripple, dip, burnout, or step.

the high-order modes can lead to a reduction of the BW. Thus we see that the step is beneficial when we are attempting to optimize the BW. Note that there are many more modes in the distribution (Fig. 6c) than there are in our closest approach to an ideal profile (Fig. 6d). In this example, the step will introduce approximately 75 more modes to the distribution as compared to the ideal profile. Figure 7 uses data obtained at $\lambda = 0.6328$ μm (A) and $\lambda = 1.32$ μm (B) to show the steps beneficial effect. Each plot represents the results for the MCVD profile with the ripple, dip, burnout, and step removed. The solid line represents N_g values for an ideal profile using the computed values of α, ΔN, and r derived from the MCVD profile, at each λ. The dashed line indicates the path taken by the high-order modes, which have been

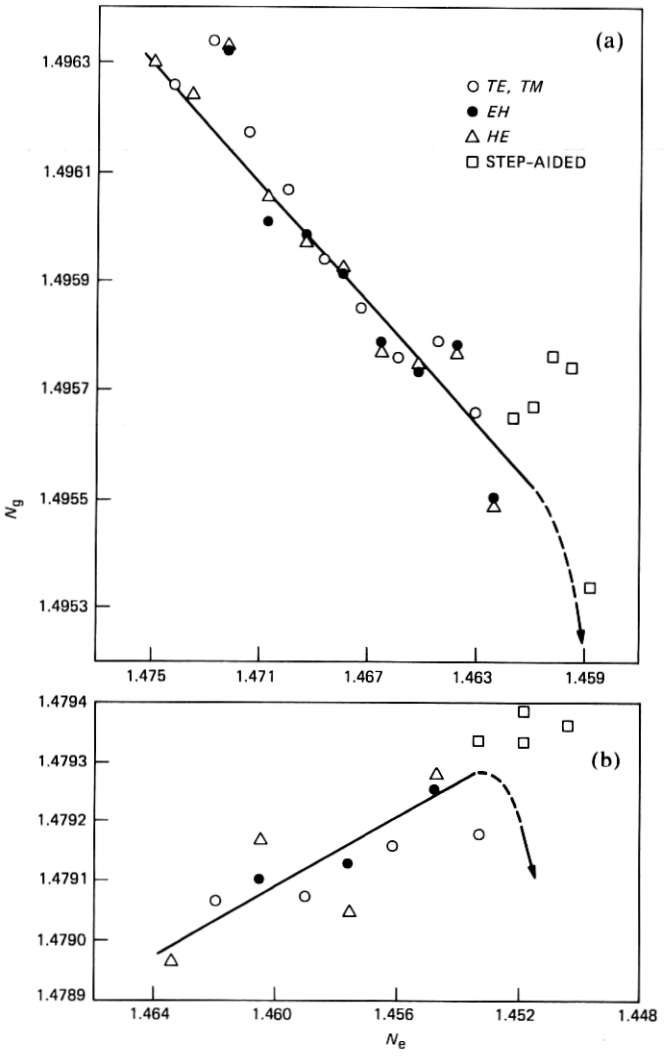

Fig. 7—N_g vs N_e. The solid line depicts an ideal profile using the pertinent parameters derived from the MCVD profile. (a) $\lambda = 0.6328$ μm. (b) $\lambda = 1.32$ μm.

altered by their proximity to the cladding. The filled squares in each plot show the N_g of some of these altered modes if the step is retained. Since this is the region of high modal density, the squares represent an addition of $\approx$100 modes to the modal distribution at $\lambda = 0.6328$ μm and $\approx$50 additional modes at $\lambda = 1.32$ μm. These additional modes can only be helpful when we are trying to optimize BW at any λ. We can now predict that the BW at these two λ's would be a function of the slope of the line.[4]

III. DISCUSSION

In our earlier work,[4] we have established that for a fixed profile that is a function of α, ΔN, and r, a least squares linear fit of N_g vs N_e, ignoring the high-order modes, will show an increasing slope for increasing λ. At a given λ, we have defined α_{opt} as that α which produces a slope of zero. A slope of zero will generate the minimum spread in N_g, in the group velocities (V_g), and of course, in the delay times. Using that criterion we can see[1] that this MCVD fiber should have an optimum operating wavelength (λ_0) of about 1.00 μm. Independent BW measurements[9] have established a BW performance of $\approx$1.5 GHz·km over the range

$$1.06\ \mu\text{m} \leq \lambda \leq 1.35\ \mu\text{m}$$

with a maximum of $\approx$2 GHz·km at $\lambda = 1.23\ \mu$m. We have reproduced the output pulse displays from this work in Fig. 8. In this figure the number in each plot is the λ in μm at which the distribution was obtained. A study of these distributions shows at least two peaks (broadening) at the short λ's, which appear to merge as λ increases. In all the pulses we see the common characteristic of a trailing tail. This tail is generated by the slowest modes in the modal distribution; at $\lambda = 0.7\ \mu$m (Fig. 6a) these would be the *low-order* modes, while at $\lambda = 1.55\ \mu$m (Fig. 2c) these would be the *high-order* modes. In Fig. 7, we have shown that the step at the core-cladding interface slows down the modes by raising the group indices. We have not attempted to derive the optimal step to optimize the BW for this profile. The reader should bear in mind that *all* modes will also be slowed down by increasing α.

In the "as is" section of this report (Section 2.1) we have seen that the burnout displaces the *HE* modes from all other modes and that the two modal groups will travel in parallel but be displaced in time. This will lead to at least two peaks in the output pulse shapes. Further, we have noted that the displacement in time will decrease as a function of increasing λ. This naturally suggests that the two peaks should merge (depending on instrumental resolution) in the output pulse of λ is increased (see Fig. 8).

IV. REDUCTION OF DATA

We now consider the separation of the various modal groups at several λ's (Table I) for the three conditions:

1. As is (includes burnout)
2. Inverted burnout (overcompensation)
3. No burnout,

and, for 2 and 3 above, the rest of the profile remains unaltered. Thus we are concerned here only with the index of refraction dip at the core

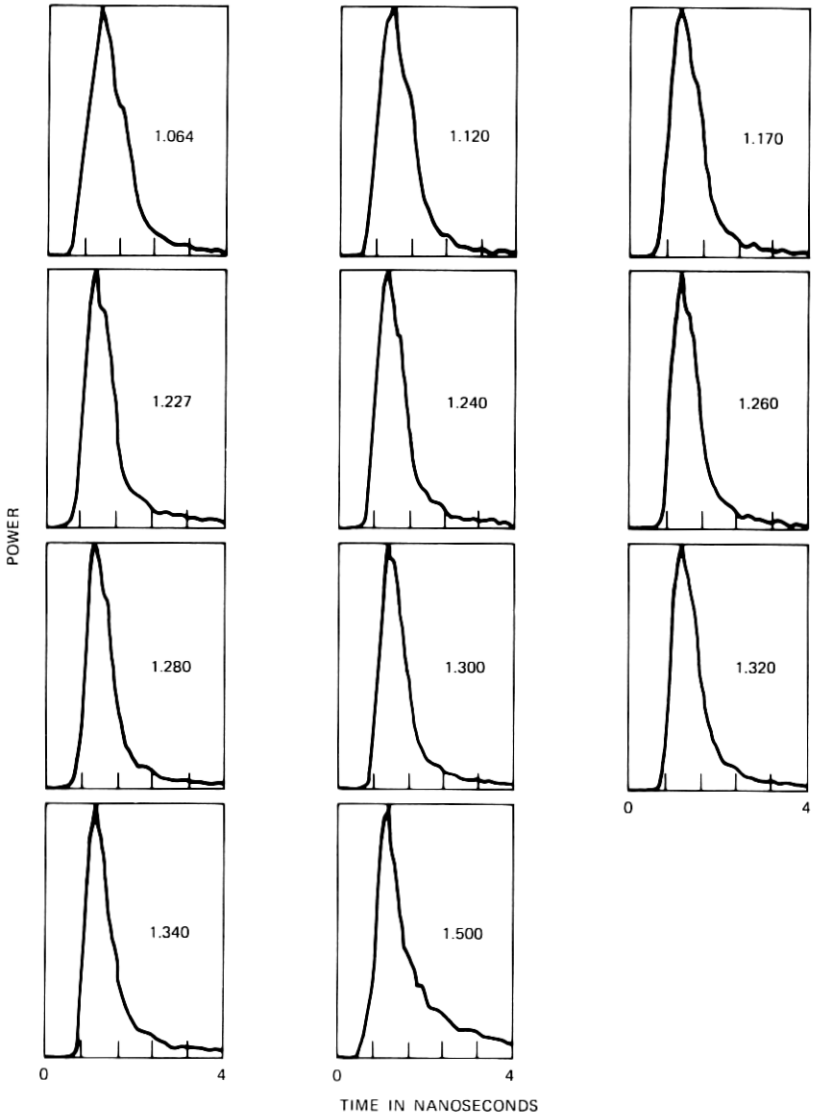

Fig. 8—Power vs time, as a function of the λ (μm) listed in each plot, for the specific MCVD fiber used in this study. Reprinted here, with permission, from Ref. 9.

center. We have previously stated that the separation of the modal groups appears to decrease for increasing λ, and this is true for 1 and 2 above. No such pattern was detected for the no burnout case. To codify these results over the range of λ's listed in Table I, we did the following.

At all λ's tested (Table I, Figs. 2a through 6a) we could generate at

least five distinct *EH-HE* splittings. We therefore found the average splitting ($\overline{\Delta N}_g$) over the first five such splittings at all λ's for each of the three cases listed above. These results are displayed in Fig. 9 as a function of λ. In the figure, the curves are defined as follows:

(A) Inverted burnout—*EH* modes separated from and moving slower than the comparable *HE* modes;

(B) As is—i.e., with burnout. *HE* modes separated from and moving faster than the comparable *EH* modes;

(C) No burnout—no real separation of modal groups—probably a random fluctuation about some relatively small average;

and 30 on the $\overline{\Delta N}_g$ axis is ≈1 ns.

Overcompensation (Curve A) is about 50 percent more deleterious in inducing splitting and is always worse in that respect than the burnout (Curve B). Further, if both phenomena are present, then the

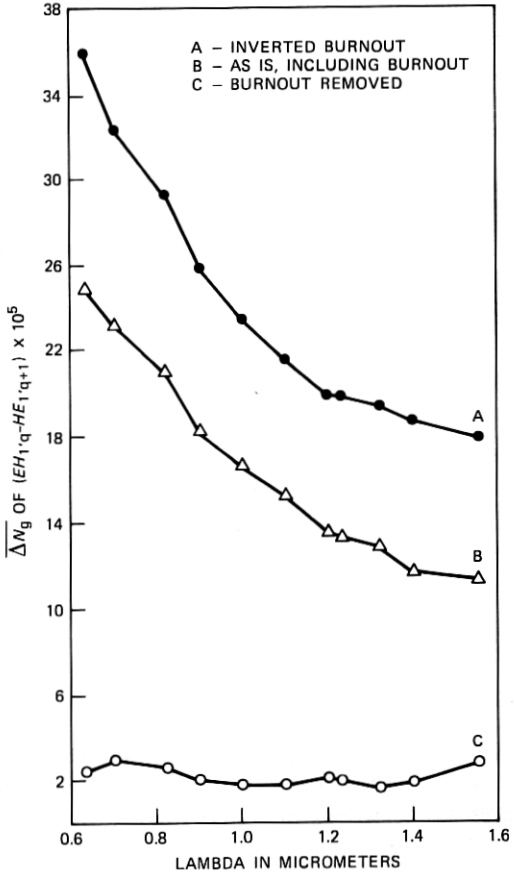

Fig. 9—The average splitting of N_g for the first five *HE-EH* modes, plotted as a function of λ, for the MCVD profile. The measurement 30 on the y axis is ≈1 ns.

total splitting is the sum of the two curves. Three distinct peaks (or more) can be produced in the output pulse of the fiber, and these modal groupings might be, among others:

1. *HE*
2. *EH*
3. *TE, TM*
4. MIXED (*HE, EH*).

In practice, preform makers[8] do not consider preforms that show significant overcompensation for fiber drawing. Experience has shown that this perturbation in the profile yields poor BW in drawn fibers.

Removal of the burnout (Curve C) has reduced the splitting of the *EH-HE* modes to a minimum that is constant over the full range of λ's investigated. This residual splitting can now be attributed to the perturbations still present in the profile, ripple, dip, and short-term ΔN_e, $\Delta\alpha$ variations, etc. If this condition could be realized in practice, i.e., burnout eliminated, the BW at each λ would be a function of α_{opt}.[4]

In our computational method,[2] we obtain the eigenvalues (N_e) at three closely spaced wavelengths, where

$$\lambda_1 < \lambda_2 < \lambda_3,$$

and λ_2 is the operating wavelength. The eigenvalues are inserted in the numerical derivative to obtain the group indices for λ_2 by

$$N_{g_2} = N_{e_2} - \lambda_2 \left| \frac{N_{e_1} - N_{e_3}}{\lambda_1 - \lambda_3} \right|.$$

Errors in the determination of N_e can be cancelled or amplified in the above formula. Thus we chose to obtain the average splitting in effective index ($\overline{\Delta}\overline{N}_e$) only at λ_2. The analogous display to Fig. 9 for $\overline{\Delta}\overline{N}_e$ is given in Fig. 10. In the figure, curves A, B, and C have the same connotation as before. We observe qualitatively the same trends for $\overline{\Delta}\overline{N}_e$ as for $\overline{\Delta}\overline{N}_g$ in Fig. 9. This information may be of some use to those computational methods[10] that calculate N_g directly from N_e.

V. CONCLUSION

We have examined the effect of various perturbations on the BW of an MCVD prepared fiber. We conclude that the primary reason for the deterioration of the BW in the MCVD as is profile is caused by the severe change in refractive index at the core center. This defect produces modal groupings that are displaced in time by as much as 0.5 ns, more or less, depending on the operating wavelength (λ_0). Short λ's are particularly sensitive to this defect, but even for longer λ's, the burnout will seriously affect attempts to maximize the BW. If burnout is minimized or eliminated in the MCVD process, we believe the next most important goal should be to optimize α at λ_0. Eliminating local

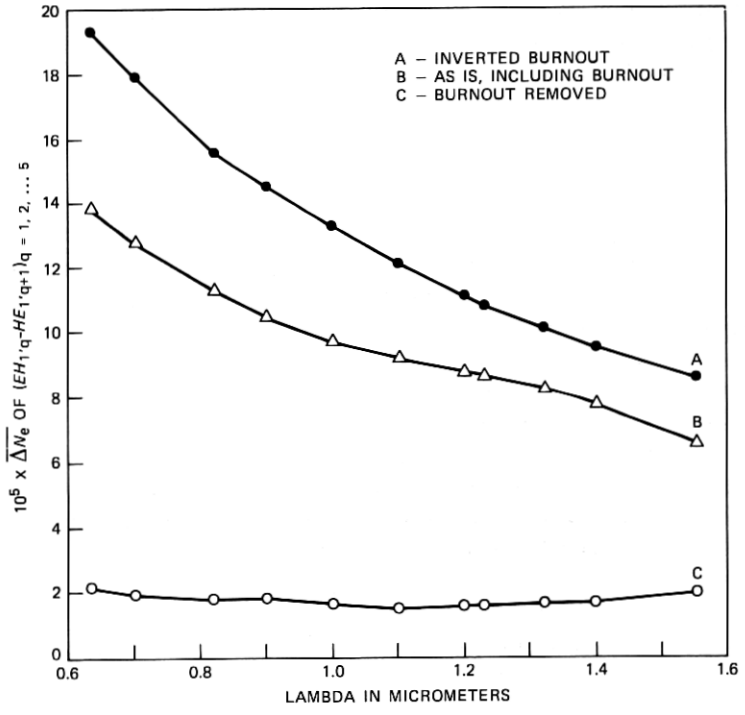

Fig. 10—Same as Fig. 9, except this is for the effective indices at the plotted λ.

shifts in ΔN would be the next priority, followed by reducing the amplitude of the ripples. This last is probably the least harmful in causing deterioration of BW. The step at the core-cladding interface appears to be beneficial in that it significantly *reduces* the number of high-order modes that have been altered by their proximity to the cladding. The works of Vassel[11] suggest that a perpendicular rise in the index of refraction at the core-cladding interface will have the same effect as the step (D) in Fig. 1.

In theory,[1,4] this MCVD fiber should have a maximum BW at $\lambda_0 \approx 1.00\ \mu m$. The experimental λ_0 was determined[9] to be 1.23 μm, and this shift to the longer λ_0 was verified by the statistical study conducted in Ref. 1. In an ideal profile, the governing factor for the optimization of BW is the determination of α_{opt} for λ_0.[4] In the MCVD profile this criterion has been overridden by the excessive broadening of the output pulse induced by the burnout causing the theoretical λ_0 to shift longer λ's. Even at longer λ's the effect of the burnout on BW is significant and may preclude the optimization of BW beyond the present state of the art.

Optimization of BW, based on optimum parameters (α_{opt}, ΔN_{opt}, etc.) derived from theoretical (ideal) concepts, will have limited appli-

cation to MCVD fibers. This limited applicability can explain to a great extent why workers in the field endeavoring to optimize BW utilizing concepts based on the theory cannot reproduce these bandwidths.

The literature is replete with studies of the effects on BW caused by disturbances in the profile such as burnoff, ripple, and steps in the index of refraction at the core-cladding interface. Most of these studies (including the present work) describe a cause and effect relationship. We are not aware of any study correlating these effects in terms of local changes in the α value, which the burnoff and/or ripples cause, resulting in a deterioration of the BW.

In our most recent work, we have tried to determine the fundamental cause of mode splitting. In this project we believe we have been successful. The fundamental cause of mode splitting is easily applied to the width and depth of the burnoff, and to the width (variable or otherwise), amplitude, and frequency of the ripples. The project is incomplete at this time.

VI. ACKNOWLEDGMENTS

This work was supported by P. A. Fleury, M. I. Cohen, R. J. Klaiber, and L. S. Watkins. We are encouraged by the enthusiasm of the materials scientists engaged in the lightguide program at Bell Laboratories, Murray Hill and Atlanta, and at the Engineering Research Center (ERC), Western Electric Co., Princeton. We are indebted to the computer personnel at ERC, Western Electric Co., Princeton, without whose strong support and cooperation this task would not have been completed.

REFERENCES

1. A. Carnevale, and U. C. Paek, "Modal Structure of an MCVD Optical Waveguide Fiber," B.S.T.J., *62*, Part 1 (July-August 1983), pp. 1415–31.
2. G. E. Peterson, A. Carnevale, U. C. Paek, and D. W. Berreman, "An Exact Numerical Solution to Maxwell's Equation for Lightguides," B.S.T.J., *59*, No. 7 (September 1980), pp. 1175–96.
3. G. E. Peterson, A. Carnevale, and U. C. Paek, "Comparison of Vector and Scalar Modes in a Lightguide with a Hyperbolic Secant Index Distribution," B.S.T.J., *59*, No. 9 (November 1980), pp. 1681–91.
4. G. E. Peterson, A. Carnevale, U. C. Paek, and J. W. Fleming, "Numerical Calculation of Optimum α for a Germania-Doped Silica Lightguide," B.S.T.J., *60*, No. 4 (April 1981), pp. 455–70.
5. U. C. Paek, G. E. Peterson, and A. Carnevale, "Dispersionless Single-Mode Lightguides with α Index Profiles," B.S.T.J., *60*, No. 5 (May-June 1981), pp. 583–98.
6. U. C. Paek, G. E. Peterson, and A. Carnevale, "Electromagnetic Fields, Field Confinement, and Energy Flow in Dispersionless Single-Mode Lightguides With Graded-Index Profiles," B.S.T.J., *60*, No. 8 (October 1981), pp. 1727–43.
7. L. S. Watkins, "Laser beam refraction traversely through a graded-index preform to determine refractive index ratio and gradient profile," Applied Optics, *18* (July 1, 1979), pp. 2214–22.
8. S. R. Nagel, K. L. Walker, and S. G. Kosinski, private communication.
9. L. G. Cohen, and S. Jang, unpublished work.

10. T. Lenahan, "Calculation of Modes in an Optical Fiber Using the Finite Element Method and EISPACK," B.S.T.J., *62*, No. 9, Part 1 (November 1983).
11. M. O. Vassel, "Calculation of Propagating Modes in a Graded-Index Optical Fibre," Opto-Electron, *5* (1974), p. 271.

AUTHORS

Anthony Carnevale, B.S. (Physics), 1960, Fairleigh Dickinson University; Bell Laboratories, 1969—. At Bell Laboratories, Mr. Carnevale has been engaged in work on nuclear magnetic resonance, electron paramagnetic resonance, and computer software. For the last four years, his work has been devoted to fiber optics.

Un-Chul Paek, B.S. (Engineering), 1957, Korea Merchant Marine Academy, Korea; M.S., 1965, Ph.D., 1969, University of California, Berkeley; Western Electric, 1969—. At the Western Electric Engineering Research Center, Princeton, N. J., Mr. Paek has been engaged primarily in research on laser material interaction phenomena and fiber optics. Member, Optical Society of America, American Ceramic Society, Sigma Xi.